Multifunctional nanoscale strategies for enhancing and monitoring blood vessel regeneration

Eunna Chung[a,1], **Laura M. Ricles**[a,1], **Ryan S. Stowers**[a], **Seung Yun Nam**[a,b], **Stanislav Y. Emelianov**[a,b], and **Laura J. Suggs**[a,*]

[a]Department of Biomedical Engineering, The University of Texas at Austin, 1 University Station, C0800, Austin, TX 78712-0238, USA

[b]Department of Electrical and Computer Engineering, The University of Texas at Austin, Austin, TX 78712-0238, USA

Abstract

Nanomedicine has great potential in biomedical applications, and specifically in regenerative medicine and vascular tissue engineering. Designing nanometer-sized therapeutic and diagnostic devices for tissue engineering applications is critical because cells experience and respond to stimuli on this spatial scale. For example, nanoscaffolds, including nanoscalestructured or nanoscale surface-modified vascular scaffolds, can influence cell alignment, adhesion, and differentiation to promote better endothelization. Furthermore, nanoscale contrast agents can be extended to the field of biomedical imaging to monitor and track stem cells to better understand the process of neovascularization. In addition, nanoscale systems capable of delivering biomolecules (*e.g.* peptides and angiogenic genes/proteins) can influence cell behavior, function, and phenotype to promote blood vessel regeneration. This review will focus on nanomedicine and nanoscale strategies applied to vascular tissue engineering. In particular, some of the latest research and potential applications pertaining to nanoscaffolds, biomedical imaging and cell tracking using nanoscale contrast agents, and nanodelivery systems of bioactive molecules applied to blood vessel regeneration will be discussed. In addition, the overlap between these three areas and their synergistic effects will be examined as related to vascular tissue engineering.

Keywords

Introduction

The field of **nanomedicine** and nanoscience has developed rapidly over the past few years. Nanomedicine applies and incorporates nanotechnology to medicine and takes the fields of biology, chemistry, and medicine down to the nanometer scale, where many biological

[*]Corresponding author. Tel.: +1 512 232 1671; fax: +1 512 471 0616. enchung@utexas.edu (E. Chung), laura.ricles@utexas.edu (L.M. Ricles), laura.suggs@mail.utexas.edu (L.J. Suggs).
[1]Authors equally contributed to produce this work.

phenomena occur. Biological processes can be monitored, controlled, and better understood through the use of nanomedicine. Current research in the field of nanomedicine has focused on therapeutic and diagnostic approaches (such as the development of nanometer-sized drug delivery systems and the use of imaging utilizing nanometer-sized particles as contrast agents), as well as on regenerative medicine and tissue engineering (such as implants, scaffolds, and biomaterials which incorporate nanoscale modifications). In addition, there are currently a number of nanotechnology-based products on the market (or in pre-market trials) and used clinically. These products span the areas of drug delivery (*e.g.* Abraxane for cancer therapy and Pegasys for Hepatitis C), *in vitro* diagnostics (*e.g.* Verigene® ID), biomaterials (*e.g.* Vitoss™ bone graft substitute and Acticoat antimicrobial barrier dressing), and nanoparticle (NP) formulations for *in vivo* and *in vitro* imaging (*e.g.* Feridex iron NPs) [1].

Biomedical imaging is the spatial and temporal visualization and monitoring of biological processes for diagnostic and therapeutic purposes. Nanomedicine has been applied to biomedical imaging applications with nanoscale control over contrast agents. There are numerous biomedical imaging modalities which are used for clinical and research purposes. Current biomedical imaging modalities include X-ray, computed tomography (CT), magnetic resonance imaging (MRI), nuclear medicine (*e.g.* positron emission tomography (PET) and single-photon emission computed tomography (SPECT)), ultrasound imaging, optical imaging (*e.g.* fluorescence, optical coherence tomography, and Raman spectroscopy), and hybrid imaging (*e.g.* photoacoustics). The choice of the biomedical imaging modality is strongly dictated by the application and the information which is desired. Each imaging modality has advantages and disadvantages and, as a result, is capable of providing different information (such as anatomical *vs.* physiological information). The ideal imaging modality should be capable of performing noninvasive, longitudinal imaging in order to monitor disease and therapeutic processes over time. For example, numerous research groups, including ours, have demonstrated that biomedical imaging technologies can successfully monitor widely used stem cell types, such as bone marrow-derived mesenchymal stem cells (BMSCs) and adipose-derived stem cells (ADSCs), *in vivo* to better understand their role in tissue engineering applications [2–5]. In addition to longitudinal imaging capabilities, the ideal imaging modality should also have sufficient contrast and resolution, as well as high signal-to-noise ratio. Most importantly, the imaging modality should be safe for the patient; any contrast agents that are used should also be non-toxic and biocompatible.

Nanotechnology applied to regenerative medicine is a cutting-edge therapeutic approach with the intent to heal diseased or damaged tissue by utilizing biomaterials fabricated at nanometer-scale level (1–100 nm) to deliver cells and/or bioactive molecules. To monitor and promote tissue regeneration efficiently, the fabrication of the biomimetic fine structure has been shown to have an important role in controlling the delivery of cytokines or cells. As well as providing chemical cues for a defined duration, these nanomaterials can be developed with the dual function to trace biological activities of labeled cells and visualize the scaffold itself.

Vascular tissue engineering may span the spectrum from large-scale blood vessel substitutes greater than 6 mm to inducing microvasculature or neovascularization processes

inside or near scaffolds. To generate blood vessels, numerous strategies such as nanoscale solid materials (*e.g.* electrospun random/aligned/core-shell nanofibers), cellencapsulated natural gels (*e.g.* fibrin gel), and chemically or physically surface-modified vascular grafts have been developed. Even though the design needs are different depending on blood vessel types, specific requirements in engineering functional blood vessels are: (1) have appropriate mechanical strength and elasticity under physiologic blood flow, (2) induce or maintain endothelial coverage to control diverse physiological signals, such as anti-thrombosis, and (3) enable blood vessel remodeling in response to stimulatory cues. In addition to biomaterial engineering strategies, diverse cell sources (*e.g.* stem cells, progenitor cells, and differentiated cells) for vascular tissue engineering have been evaluated for their regeneration potential. Vascular cells such as endothelial cells (ECs) and smooth muscle cells (SMCs) can be derived in the adult from stem cell populations that may include mesenchymal stem cells (MSCs) [6,7], ADSCs [8,9], endothelial progenitor cells (EPCs) [10], and others [11]. Cell functions important in vascular tissue engineering include proliferation/differentiation potential, paracrine activity for angiogenesis, and migration. Recently, numerous nanotechnology strategies, as described above, have been applied to visualize and regenerate blood vessels. In the current review, we summarized current advances in regenerative nanomedicine targeting vascular tissue regeneration focused on microvessels and also suggest next-generation nanomedicine techniques, which can be applied to reconstruct blood vessels as shown in Fig. 1.

Nanoscaffolds for vascular tissue engineering

Nanoscale-structured vascular scaffold

The importance of nanoscale features in vascular tissue engineering scaffolds has been recently demonstrated as a means of more accurately recapitulating the extracellular matrix (ECM). The ECM is a composite of nanofibers on the order of 5–500 nm in diameter [12]. The fibers are primarily composed of collagens and elastins that are decorated with nanoscale adhesive proteins such as laminin and fibronectin [13]. The ECM is highly instructive to the cells, and has been shown to direct or regulate cell shape, growth, migration, and differentiation [14]. Tissue engineers have focused on developing techniques to produce nanoscale features within scaffolds, which can be defined as nanoscaffolds, in order to replicate the ECM structure. Nanofiber scaffolds are three-dimensional constructs with an interwoven, porous architecture. Zhang et al. [15] reported on a nanostructured (200–400 nm) scaffold based on the natural polymer fibrin. This gel-type scaffold included nanofibers and showed greater mechanical properties by chemical modification (*i.e.* PEGylation), capable of more stable tube-like networks of seeded cells. The fibers can be either natural or synthetic and are generated using a variety of techniques such as electrospinning or phase separation. In addition, nanopatterned scaffolds have specific topographical features for cell instruction. These scaffolds are designed to mimic the topography found in the basal lamina. Table 1 shows recent vascular tissue-related nanoscaffolds and their results.

Electrospinning is one of the most controlled, easy, and popular methods to make a nanofibrous scaffold in tissue engineering. Fibers are formed by releasing a solution through

a syringe into a rolling collector under an electric field. Using electrospinning, fiber characteristics such as size, orientation, structure (*e.g.* solid, core-shell, porous, and spiral) and incorporation strategies with bioactive molecules can be controlled [16]. Numerous synthetic polymers such as PLGA, PCL, and PLCL, and natural biomaterials (*e.g.* collagen, elastin, and fibrin), and combined biomaterials of synthetic and natural polymers have been chosen to form ECM-mimicking nanostructures in tissue-engineering devices. While the nanofibrous structures of natural polymers, such as fibrin, are driven by characteristics of those proteins, we can still engineer them with controlled and well organized structures. Perumcherry et al. demonstrated that PVA-mediated electrospinning techniques were applied to fibrinogen and thrombin using a dual-syringe system [17]. This system was capable of generating controllable nanofibers from 50–500 nm, upon which MSCs can adhere, spread, and proliferate [17]. Moreover, in vascular tissue engineering, enhancing EC activity, such as adhesion, alignment, growth, and differentiation, is a critical aim for successful blood vessel regeneration. Hajiali et al. utilized a combined polymeric nanofiber platform, which was fabricated by electrospinning using synthetic (PGA) and natural (gelatin) polymers, for vascular cell cultivation [18]. Depending on the gelatin concentration combined with PGA, the nanofiber scaffolds had varied effects on different mechanical properties and varied effects on SMC and EC responses [18]. Electrospun fibers have been successfully incorporated as the intimal surface of a larger vascular graft. However, it remains challenging to generate electrospun fiber constructs with high porosity to allow for deep cell migration in a thick 3D scaffold. As electrospinning technology progresses, we anticipate solutions to this problem will be developed with a variety of natural and synthetic materials.

In addition to electrospinning, phase separation also can generate nanofibers. Natural ECM-like PLLA nanofibers (50–500 nm) were fabricated by liquid–liquid phase separation and a low temperature-gelation technique [19]. These nanoscale structures in this biodegradable scaffold with large porosity may improve adherence and growth of blood vessel cells by providing a more conducive environment.

Self-assembly (SA) is an attractive technique for the production of fibers down to 5 nm with incorporated bioactive moieties [20]. The Stupp laboratory pioneered the field with peptide amphiphiles which are created with four basic functional units; (1) a hydrophobic moiety, (2) a β-sheet forming unit, (3) a series of charged amino acids, and (4) a bioactive molecule [21]. Each functional unit can be tuned to fit a particular application; for example, the β-sheet unit is responsible for most of the mechanical properties, gelation kinetics, and structure. This strategy has been employed to produce fibers as small as 6 nm in diameter and up to several micrometers in length, with elastic moduli on the order of 10 kPa [22]. For vascular tissue engineering applications, Rajangam et al. suggested heparin-binding (consensus) peptide amphiphile SA gels as an EC-adhesive nanostructured platform, which also can deliver angiogenic growth factors such as vascular endothelial growth factors (VEGFs) [23].

In addition, Jung et al. demonstrated that an advanced SA peptide hydrogel system could enhance EC activities (proliferation or CD31 expression) through chemical modification, including β-sheet ligation and RGD addition [24]. Similarly, Cho et al. showed a self-assembled nanofibrous scaffold, which contained an RGD-like motif, RAD peptides

(RAD16-II=AcN—RARADADARARADADA—CNH$_2$), enhanced angiogenesis with VEGF up-regulation in wounded tissue [25]. The authors suggested that a weaker interaction between ECs and RAD peptides via the β_3 integrin/MAPK/ERK pathway compared to RGD could allow for greater EC migration [25]. Sangnella et al. showed that the RGD content in a polymeric complex, which consisted of backbone poly(vinyl amine) connected with RGD peptides and oligosaccharides (maltoheptose), influenced EC behavior and proliferation [26].

In addition to adhesive peptide molecules, biomolecules such as matrix metalloproteinases (MMPs), which are involved in angiogenesis, can be incorporated into the scaffold. Tambralli et al. developed PCL nanofibers in which the outer layer was covered by self-assembled MMP2-sensitive sequences and RGD-peptides [27]. This construct demonstrated improved cell adhesion and spreading [27]. Moreover, nanofiber gels were created from ionic self-complementary peptides in a study by Narmoneva et al. [28]. Cardiomyocytes were seeded in these gels alone, with ECs, or in gels that had been prevascularized by ECs for 24 h prior. Co-culture with ECs promoted the formation of proper cell—cell junctions between the cardiomyocytes. The prevascularized gels increased spontaneous contractility of the cardiomyocytes by three orders of magnitude over controls, demonstrating a functional enhancement. In a later study, the nanofiber gels injected into the myocardium of mice were shown to recruit ECs and SMCs that were found in *de novo* vasculature [29]. Taken together, a scaffold composed of self-assembled nanoscale fibers with chemical and geometric cues can be beneficial for neovascularization.

Nanoscale surface-modified vascular scaffold

Nanopatterning for vascular applications seeks to mimic the topography of the basal lamina to direct cell behavior. In Lu et al.'s study, diverse nano- and micro-scale surface modifications of titanium were investigated to compare EC attachment and growth [30]. The uniform nano-patterned surfaces with linear grooves (750 nm) showed greater EC adhesion and growth than larger surface patterns or random nanoscale modification. Similarly, to enhance EC coverage, Fine et al. developed a nanotube-coated titanium stent [31]. Self-assembled Rosette nanotubes have a nanoscale helical structure that is stabilized by hydrogen bonded stacks similar to those between DNA bases, *i.e.* guanine and cytosine (GC motif), and includes an amino acid (lysine) side-chain. This study demonstrated that the biomimetic nanosurface of the vascular stent enhanced adhesion and growth of ECs [31]. Moreover, Dalby et al. created nanoscale islands on polystyrene with heights of 13, 35, or 95 nm [32]. ECs adopted a more spread morphology on these surfaces compared to on smooth surfaces. The 13 nm islands produced the largest difference in morphology. According to Wang et al. [33], the nanopatterned structure of a PLGA scaffold influenced EC adherence and proliferation, showing greater levels of cellular activities on a less rough surface (20 nm) compared to a more rough surface (80 nm). In addition to the EC-based studies, in a study by Yim et al., SMCs showed more stretched and aligned cell shapes on nanopatterned PMMA and PDMS, depending on the matrix topography, in spite of their decreased proliferation tendency [34]. In another study by Miller et al., enhanced densities of both cell types (*i.e.* SMC and EC) were shown on the polymeric PLGA sheet that was not regularly grooved but contained varied nanotopographies [35]. Chung et al. produced nanoscale

roughness on polyurethane films by coating them with RGD-conjugated polyethylene glycol (PEG) molecules with either uniform or varied chain lengths [36]. Human umbilical vein endothelial cells (HUVECs) adhered and proliferated more rapidly on the rough films with varied chain length [36]. In addition, combining preconstructed artificial blood vessels in a 3D natural gel can be accomplished using nanoscale surface manipulation with bioactive molecules. In Hadjizadeh et al.'s recent report, ECs were cultured on 100 μm thick poly(ethylene terephthalate) fibers whose surface contained RGD sequences [37]. The EC-aligned RGD-nanofibers embedded in a fibrin gel showed superior guidance and good connection with ECs in a fibroblast co-culture system [37].

Bettinger et al. investigated EPC activity on a PDMS-collagen substrate with nanogrates of 600 nm width and 1200 nm periodicity [38]. EPCs exhibited elongated and aligned morphology while migrating faster on nanograted materials compared to smooth surfaces, but there were no significant differences observed in gene expression, indicating that topography is only a component of enhancing vascular regeneration [38]. Liliensiek et al. sought to determine the effects of anisotropic surface topography on a variety of ECs [39]. Anisotropic ridge and groove structures or isotropic pores were created in polyurethane, and vascular cell types from different origins were cultured. Anisotropic features increased alignment and migration compared to isotropic pores, and the response was dependent on the anatomic origin of the EC to an extent.

Understanding the effect of nanoscale topography *in vitro* is critical to developing a model of cell behavior in vascular environments. *In vitro* studies should be extended into animal models in the future to investigate the functionality of these advances. It is also necessary to develop fabrication methods that allow for nanotopographical cues to be incorporated into a variety of tissue engineering constructs.

Nanoscale imaging and cell labeling

Biomedical imaging, which is defined as the visualization and monitoring of biological process for diagnostic and therapeutic purposes, is essential for tissue engineering applications. To evaluate tissue regeneration properly, it is imperative to monitor and track these therapies over time *in vivo* by visualizing vascular formation or tracking cells used for cell-based therapies. Various types of imaging analysis can be employed to gather this information. Several other reviews have discussed and compared in depth the imaging modalities for cell tracking purposes [40,41]. The first technologies to utilize nanocontrast agents were nuclear-based techniques such as SPECT and PET. Since then, researchers have begun to appreciate the importance of designing contrast agents on the nanometer scale. In this section we will focus on strategies using contrast agents which are designed and engineered on the nanoscale to be used for tissue engineering applications. Specifically, applications of nanocontrast agents related to *in situ* labeling (*i.e.* intravenously injecting nanocontrast agents which can either passively label vasculature or specifically target and label cells) and cell pre-labeling (*i.e.* labeling cells with nanocontrast agents which are then injected) will be discussed. Various examples of these contrast agents and labeling techniques are described below and are outlined in Table 2.

In situ labeling and vascular imaging

In situ nanoscale vascular imaging involves intravenously injecting nanocontrast agents in order to visualize vessels. The nanocontrast agents can nonspecifically label vasculature or can target cells with specific surface markers. Vascular imaging, such as angiography, is used clinically to diagnose the status of blood vessel networks or vascular interventions. In tissue engineering, in particular, visualization and evaluation of blood vessel regeneration is still being pioneered. A variety of imaging techniques that were developed or used in other fields such as cancer have been used to evaluate neovascularization in scaffolds near damaged tissue. Vascular casts [42] and histological techniques [43] are commonly used to evaluate blood vessels, and detection can be improved by staining for specific endothelial cell markers. However, implementing noninvasive imaging techniques would be desirable for evaluating growing vascular networks. Current noninvasive angiographic techniques which are used clinically can only evaluate relatively larger vessels and patients are usually exposed to ionizing radiation and contrast agents [44]. Thus, for tissue engineering applications, using imaging modalities with or without contrast agents which are capable of monitoring blood vessels, and specifically microvessels, is imperative. Many investigators have implemented novel techniques using nanocontrast agents in order to assess cell-based therapies for vascular regeneration. It is possible to visualize smaller vessels using nanoscale contrast agents because of increased sensitivity and the ability to implement complementary imaging modalities.

Recently, investigators have explored the application of nonspecifically injecting magnetic NPs into the vasculature in order to enhance the visualization of the vessels [45,46]. Howles et al. used magnetic resonance angiography and employed a nanoscale modified gadolinium system (75.9 nm), in which gadolinium was immobilized on the surface of a liposome, providing increased contrast and a larger field of view for imaging small blood vessels in the body (see Fig. 2A(i)) [47]. Lu et al. used 40 nm hollow gold nanospheres to enhance the sensitivity for brain vascular imaging using photoacoustic tomography [48]. The NPs greatly enhanced contrast and provided visualization of vessels as small as ~100 μm in diameter [48].

In addition to obtaining structural information, assessing vascular networks in terms of functional characteristics is also important. Towards this end, tissue engineering can use the advantage of actively targeting nanoscale contrast agents to angiogenic vessels in order to distinguish them from surrounding vascular networks and to better evaluate their maturity. Targeting the $\alpha_v \beta_3$ integrin is ideal for detection of angiogenesis because only very low levels are expressed in normal vessels [49]. Winter et al. imaged perfluorocarbon NPs targeted to $\alpha_v \beta_3$ integrins using MRI in an ischemic animal model in order to evaluate the angiogenic therapeutic effects of L-arginine [49]. L-arginine treated animals showed more extensive angiogenesis and thus MRI signal enhancement compared to sham treated animals [49]. In a study by Smith et al., RGD-quantum dots (QDs) (6–8 nm in diameter) were specifically targeted to newly formed blood vessels expressing $\alpha_v \beta_3$ integrins, and the QDs were found to bind significantly more often to tumor vessel endothelium than in normal tissues (see Fig. 2A(ii)) [50]. The imaging techniques outlined in this section, which incorporate nanocontrast agents, allow for the visualization of microvessels in the early

stages of therapy, which cannot be achieved with other imaging modalities, such as angiography.

Cell pre-labeling and imaging

Optical labeling—Engineered nanocontrast agents for optical imaging include QDs and noble metal (*e.g.* gold and silver) NPs. QDs are semiconductor NPs (usually 2–10 nm) which can be excited by a wide range of wavelengths, exhibit size-dependent tunable emission, and are relatively photostable [2,51–53]. Lin et al. demonstrated *in vivo* multiplex imaging of mouse embryonic stem cells (ESCs) labeled with six different QDs [2]. The cells were injected subcutaneously into the backs of nude mice and imaged using fluorescent microscopy [2]. Five of the QDs were detectable up to day 2, and one of the QDs (QD 800) was detectable up to day 14 [2], thus demonstrating the feasibility of longitudinal *in vivo* imaging of stem cells labeled with QDs. In addition, So et al. presented QD conjugates which can be used for both *in vivo* fluorescence and bioluminescence imaging [52]. An eight-mutation variant of *Renilla reniformis* luciferase (Luc8) was conjugated to polymer-coated CdSe/ZnS coreshell QDs [52]. The QDs alone, as well as rat glioma cells labeled with the QDs, were capable of being imaged using bioluminescence and fluorescence imaging when injected into nude mice [52]. Designing contrast agents which are capable of being imaged with various imaging modalities can be an advantage, as outlined in the "Labeling for multimodal imaging" section below. However, a major concern with QD labeling can be toxicity, as demonstrated by Muller-Borer et al., who found dose-dependent toxicity effects for rat MSCs labeled with CdSe/ZnS QDs (10–15 nm) [53]. But, QD toxicity largely depends on physiochemical properties [54], and thus thoroughly investigating these effects is important.

Gold NPs can be made in a variety of sizes and shapes (*e.g.* spheres, rods, shells, and cages), and these intrinsic properties determine the wavelengths at which gold NPs maximally absorb and resonantly scatter light [55–57]. In addition, the core of gold NPs is inert and non-toxic to cells [55,58], and various surface coatings can be conjugated to the gold surface via thiol or amine moieties, which have well defined surface chemistries with gold [55,59]. Gold NPs are commonly used as contrast agents for cell labeling in applications related to cancer imaging, diagnosis, and therapy [60–62]. However, the use of gold NPs is also being extended to stem cell labeling and *in vivo* tracking. Previous work in our lab studied MSC function following labeling with spherical gold NPs of various sizes (20–60 nm) and surface coatings [3]. MSCs maintained the ability to proliferate and differentiate following labeling with all NP formulations [3]. Furthermore, we imaged gold NP labeled MSCs *in vivo* using combined ultrasound and photoacoustic imaging [4]. The MSCs could still be detected after 10 days, and spectroscopic imaging clearly distinguished NP labeled MSCs from surrounding tissue, including skin and blood, as shown in Fig. 2B [4]. Thus, ultrasound/ photoacoustic imaging can monitor MSCs *in vivo* and evaluate the extent of vascular regeneration following stem cell therapy. Moreover, Nagesha et al. demonstrated *in vitro* imaging of mouse ESCs labeled with 10 nm gold NPs using multi-photon photoluminescence imaging [63]. The stem cells maintained their proliferation ability following NP labeling and were imaged *in vitro* with two-photon luminescence using a wavelength of 790 nm [63]. However, using NPs to monitor cell function, such as

proliferation and differentiation, which is essential for stem cell therapies, needs to be explored further.

Magnetic labeling—Superparamagnetic iron oxide (SPIO) NPs, consisting of an iron oxide core as small as 5 nm [64,65], are commonly used, commercially available labeling agents for MRI. SPIO NPs produce negative contrast (*i.e.* the MR signal is reduced in the presence of SPIOs) [57,64,65]. Polymers such as dextran, carboxydextran, or polylysine are often used to coat SPIO NPs in order to prevent NP aggregation [59,64,65] and increase cell labeling efficiency [59,64]. Numerous studies have used MRI to monitor stem cell therapies *in vivo*. Guzman et al. tracked magnetically labeled human central nervous system stem cells (hCNS-SCs) in a stroke model using MRI and found that labeling hCNS-SCs with magnetic NPs had no effect on cell proliferation and differentiation *in vitro*, and the cells could be tracked up to 18 weeks *in vivo* and exhibited similar function as unlabeled cells [66].

A major challenge with cell therapy for vascular repair is the inability to track cells and monitor neovascularization. Towards this end, Lange et al. investigated the therapeutic usefulness of stem cell therapy for renal failure [5]. Irondextran NP labeled MSCs were infused into rats which had undergone acute renal failure. Using MRI, NP labeled MSCs were found to be in the renal cortex up to three days and renal function was significantly improved [5]. Kraitchman et al. tracked magnetically labeled MSCs in a myocardial infarction (MI) model using MRI, and found the cells were still detectable up to one week after the injection, but only 25.8% of the original hypointense lesions attributed to MSCs could be detected after three weeks [67]. Both of these studies demonstrate the advances made towards tracking cells for vascular therapy, but also indicate that work is still needed in order to conduct long-term cell tracking studies. Furthermore, in addition to detecting magnetically labeled cells, MRI can also detect ferritin deposits outside of cells or which have been endocytosed by macrophage cells. Thus, specifically detecting magnetically labeled stem cells should be further explored in order to distinguish targeted cells.

Labeling for multimodal imaging—In order to obtain an accurate description of cell tracking and tissue regeneration, it is usually necessary to gather both anatomical and functional information. However, no single imaging modality is capable of providing all these details, and thus it is usually necessary to employ multimodal imaging. To this end, many are developing labeling agents that are capable of being imaged with multiple imaging modalities. Lu et al. developed fluorescein isothiocyanate (FITC)-incorporated silica-coated core-shell SPIO NPs (SPIO@SiO$_2$(FITC)) that are capable of being imaged with MRI and fluorescence imaging [68]. The NPs efficiently labeled human MSCs without any toxic effects on cell function, and the cells could be detected using MRI when subcutaneously injected into the flanks of mice [68]. As another MSC-tracking example, Narayanan et al. reported on a green synthesis route for preparing multimodal nanohybrids based on Fe$_3$O$_4$/Au possessing magnetic and X-ray contrast properties [69]. The nanohybrids (~35 nm) did not have cytotoxic effects on human MSCs, displayed superpara-magnetism with high magnetic saturation, and exhibited CT contrast that was superior to the conventional iodinecontrast agents [69]. In addition, Patel et al. developed an ion-sensing NP comprised of a SPIO core encapsulated with a porous silica shell, which could be anchored with

ligands capable of coordinating with positron-emitting metals [70]. The SPIO@-SiO$_2$ NPs had high uptake efficiency, were not cytotoxic to the stem cells, and were comparable to commercially available Feridex in terms of MRI contrast [70].

Nanodelivery systems of bioactive molecules

Incorporating drug delivery systems into a cell/materialbased device is an attractive strategy to maximize the regenerative capacity of tissue-engineered devices. This concept of regenerative medicine is based on modifying cellular activities (*e.g.* adhesion, proliferation, differentiation, and migration) by (1) directly providing essential bioactive molecules required in the healing process, or (2) inducing seeded or neighboring cells inside or near scaffolds to produce specific proteins via DNA introduction. Nanoscale carriers, compared to microscale systems, can travel more easily into difficult locations such as the microvasculature inside tissue scaffolds or directly into cells or cell nuclei. In particular for blood vessel regeneration, these delivery strategies have been developed to incorporate target biomolecules such as adhesion molecules (*e.g.* integrins), growth factors (*e.g.* VEGF, bFGF, and PDGF), extracellular matrix (*e.g.* fibronectin and elastin), tight junction proteins (*e.g.* claudin and occludin) and signaling molecules (*e.g.* eNOS and Raf-1) [71]. Here, we will focus on recently-developed nanoscale carriers to deliver genes, peptides, and proteins related to blood vessel formation, as shown in Table 3.

Gene delivery

Delivering genes into target tissue can be accomplished by a variety of methodologies as follows: physical (*e.g.* naked or plasmid DNA injection, gene gun, and electroporation), biological (*e.g.* retrovirus, adenovirus, and adeno-associated virus), and material-based (*e.g.* liposomes, biodegradable polymeric scaffolds, and metals) [72]. Physical delivery methods have the disadvantages of low transfection and low targeting efficiency, and viral vector systems can induce mutagenesis [73]. However, with nanomaterials, bioactive molecules can be targeted, showing long-term controllable release profiles without serious safety concerns [74]. Diverse nano-biomaterials to deliver DNA and siRNA were applied as shown in Table 3.

The liposome-mediated gene delivery system, named lipoplex, is a nanosize carrier for nucleic acids without any viral vectors [75]. This system can be designed to be controlled by physical stress such as pH, ultrasound, light, and magnetic field [75]. However, a scaffold combined with lipoplex can deliver genes for a significantly longer time compared to plasmid DNA alone or in the lipoplex. In addition, this system can induce a higher level of gene transfection efficiency than scaffolds without liposomes [75]. A vascular stent with eNOS gene-*LacZ*-liposomes introduced into a damaged rabbit artery induced greater endothelial cell regeneration than liposome-coated or non-treated stent controls (28 days) [76]. Additionally, peptide-NPs delivering the hypoxia-inducible factor (HIF)-1α gene without the oxygen-sensitive degradation domain induced increased levels of VEGF gene and protein *in vitro* and better angiogenesis in a skin wound than VEGF-A$_{165}$ protein treatment [77]. Polyelectrolyte NPs can deliver a low dose of DNA (61.8 nm in 20 nM Hepes, pH 7.4) to blood vessels up to 3 days [78].

In tissue engineering, genes can be introduced using viral or non-viral agents and incorporated to the target cells or tissue environment using (1) cell transfection, (2) *in vivo* direct injection, and (3) 3D matrix incorporation [72]. The limited regenerative capacity of cell sources can be improved through mediating gene expression by introducing genes to (1) repair dysfunctional stem cells or organs and (2) induce regenerative mechanism-related or drug molecules [79]. Candidate cell sources (*e.g.* BMSCs, ESCs, EPCs, and ECs) for vascular tissue engineering can be targeted for gene delivery. Transfected cells in a tissue-engineered system can overexpress specific proteins, such as pro-regenerative growth factors. Deng et al. showed higher transfection of the TGF-β1 DNA plasmid using *Pleurotus eryngii* polysaccharide (CPEPS) NPs (~80 nm) into BMSCs without serious cytotoxicity compared to other nonviral gene delivery systems [80]. According to Yang et al.'s study, VEGF gene introduction using biodegradable poly(β-amino esters) NPs into human MSCs (hMSCs) and ESCs (hESCs) increased VEGF secretion enhancing vascularization in ischemic hind limbs [81]. Similarly, Zhu et al. delivered the human $VEGF_{165}$ gene into myoblasts using 100–500 nm NPs made of hyperbranched polyamidoamine [82]. Hyperbranched dendrimers were stable and showed low cytotoxicity similar to polyamidoamine (PAMAM) dendrimers, but could be fabricated more simply [82]. These non-viral nanodelivery particles showed higher transfection efficiency than lipofectamin or polyetherimide, protection of gene digestion via DNase I, and enhancement of blood vessel formation with anti-apoptotic effects in a mouse MI model [82].

An advanced nanoscale liposome system delivering the bFGF gene was developed to solve problems with low transfection efficiency, degradation of DNA, and diffusion limitations of prior non-viral strategies such as microbubbles and liposomes [83]. Negishi et al. reported on a cationized bubble liposome system (~523.6 nm), which included PEG surrounding ultrasound contrast gas that was capable of delivering the bFGF gene stably with better angiogenic effects following ultrasound exposure [83]. Therefore, a variety of novel strategies using nanoscale materials for gene delivery can allow functional angiogenic genes to be delivered stably into cells or injured target regions with greater bioactivity for blood vessel regeneration. However, several issues remain to be solved, including optimizing the trade-off between transfection efficiency and cytotoxicity and achieving more controlled release capabilities of multiple genes.

Protein delivery

Growth factors such as VEGF, PDGF, bFGF, TGF-β, and HGF have been applied most commonly to promote blood vessel regeneration. A VEGF nanodelivery system consisting of dextran sulfate and a polyelectrolyte complex of various polycations (*e.g.* chitosan, PEI, poly-L-lysine) was characterized with a size range of 160–280 nm and a zeta potential of −12.9 to 18.7 mV [84]. All formulations maintained significantly higher amounts of released VEGF over time than VEGF alone (without NPs) [84]. Golub et al. showed greater blood vessel formation in a mouse ischemia model by delivering VEGF in ~400 nm PLGA NPs than VEGF without any carrier [85]. In addition, mesoporous silica NPs (57 nm), which have advantages of large surface area-to-volume ratio and controllable pore sizes, were localized in the cytoplasm of HUVECs without any cytotoxicity and released bFGF over 20 days [86].

The characteristics of NPs and 3D scaffolds can control the delivery mode and timing, suggesting that the choice of the delivery system should depend on the target tissues and application purpose. In Jeon et al.'s report, star-shaped PLGA NPs of relatively low molecular weights (15 kDa) could be conjugated with heparin to control bFGF release [87]. Delivery of these particles was sustained in a density dependent manner with increasing concentration of fibrin in their composite system; 188.6 mg/ml 3D fibrin gels showed the greatest sustained release with 49% bFGF released at 4 weeks [87]. Their heparin-PLGA NPs-fibrin gel system incorporating bFGF enhanced microvascular regeneration in the ischemic limb model [87]. PLGA-poloxamer (1:1)-blended NPs were suggested as a dual growth factor carrier, demonstrating one month delivery of FGF-2 and PDGF and their mitotic effect on ECs [88]. However, even though nanoscale strategies can enhance long-term sustained release of angiogenic proteins, the regeneration process of blood vessels requires numerous growth factors and enzymes. For this, more elaborated chemical and material engineering techniques should be developed to allow multiple proteins to release efficiently within the optimal time range.

Multifunctional nanomaterials for tissue engineering

Nanoscaffolding for delivery of bioactive molecules

Nanoscaffolding as described above (see ''Nanoscaffolds for vascular tissue engineering'') can also be applied as a carrier for therapeutic bioactive molecules. Construction of biofunctional nanoarchitecture is an attractive strategy to tissue engineers in that it can not only provide the ECM-like environment familiar to seeded or host cells in the regeneration process, but also induce a localized and specific action by bioactive molecules. Electrospun nanofiber scaffolds can deliver numerous proteins, including growth factors, by various loading methodologies: physical absorption, blended or coaxial (core-shell) electrospinning, and covalent immobilization [89]. Kim et al. utilized 400–500 nm nanofibers by electrospinning a combined solution of PCL and gelatin (50:50) followed by heparin surface-modification for bFGF delivery [90]. It was shown that engineering the nanofibrous scaffolds according to different spinning gel volumes and whether or not heparin conjugation was used could modulate bFGF delivery. They demonstrated the highest HUVEC and MSC growth on day 9 with thicker heparin-modified fibers.

Novel techniques have been developed to sustain or control release of delivered molecules without an initial burst release. In Wei et al.'s report, a combination of PLGA microspheres and PLLA electrospun nanofibers showed sustained PDGF-BB release longer than 40 days. A more recent engineering technique for protein delivery applications is coaxial electrospinning, which involves fabricating multilayers of nanofibers by simultaneously injecting two isolated solutions from overlaid needles. The release of FITC-BSA [91] or PDGF-BB [92], which were loaded in the PEG center covered by a PCL outer layer, could be controlled by varying the scaffolding parameters (*e.g.* flow rate, PEG concentration, and PEG molecular weight). Moreover, Lu et al. utilized a co-axial electrospinning strategy to fabricate double-layered fibers (~3–4 μm fiber diameters), in which the cationized gelatin outer layers with immobilized heparin could play a role as a superior VEGF-releasing carrier over time (15 days) [93].

However, suitable fabrication methods may depend on the delivery purpose and target cell types. Sahoo et al. compared two different bFGF delivery methods (homogeneous mixed and core-shell type) based on electrospinning using PLGA nanofibers (200–300 nm diameter) with respect to ECM protein (collagen and fibronectin) production and proliferation of rabbit BMSCs [94] (Fig. 3A). Homogeneous blended bFGF showed a greater release ratio over 1 week and fibroblast-related gene expression than the core-loaded system [94]. Furthermore, multimodal natural gel systems have been developed to effectively control independent release of several bioactive growth factors (*e.g.* TGF-β1/PDGF-BB [95], VEGF/PDGF-BB [96]) according to their involvement in tissue regeneration. Nanocarriers can also be incorporated into nanofibrous scaffolds. According to Tan et al.'s study, VEGF at concentrations of 50 and 250 ng/ml in the solution was loaded into heparin/chitosan NPs and these NPs with VEGF were chemically immobilized into bovine decellularized nanofiber scaffolds [97]. This system induced significantly sustained release of the growth factor at levels of 37% and 42% of the initial loaded total amounts, respectively, at 30 days [97].

Hydrogels can enable genes to be targeted with sustained and controlled release profiles and also prevent DNA degradation [73]. In Breen et al.'s *in vivo* study, a fibrin gel encapsulating adenoviral vectors encoding β-galactosidase showed higher transfection activity without any significant negative effects on wound healing and vascularization relative to the viral vector only group in a rat ear ulcer model [98]. Fibrin was used to release genes, such as plasmid DNA for enhanced green fluorescent protein (eGFP) expression (*in vitro*), and β-galactosidase and luciferase (*in vivo*), in a commercially available liposome, Lipofectin® [99].

A recent advancement using SA fibers is the ability to form complex structures. Chow et al. demonstrated formation of a peptide-based membrane that permitted cell adhesion and could also bind and release growth factors [100], similar to Rajangam et al.'s study introduced earlier (see ''Nanoscale-structured vascular scaffold'') [23]. Hyaluronic acid was combined with a cationic peptideamphiphile with a heparin-binding domain to form the membrane. MSCs were shown to adhere and proliferate on the membrane. Additionally, robust angiogenesis was seen in a chick allantoic membrane assay when the membrane was loaded with small amounts of growth factors compared to unloaded membranes or soluble growth factor addition. These kinds of peptides can also be incorporated in a scaffold by immobilization on the surface or chemical modification. In Ferreira et al.'s study, ESCs did not show any significant loss of viability and expressed endothelial phenotype markers such as Tie-2, AC133, and CD31 in an RGD peptide or VEGF-incorporated dextran matrix [101].

Combined imaging and delivery nanoscale systems

A variety of bioengineered nanoscale strategies with the dual functionality of sensing/imaging and drug/gene delivery have been developed, particularly in cancer therapy. That is, many have demonstrated the application of encapsulating drugs in NPs, delivering them to cancer cells, and determining if the NPs were delivered to the tumor site. Furthermore, it is possible to determine that these drugs have performed their intended function by imaging the particles *in vivo* with various imaging modalities [61,102]. However, extending the multi-functionality of delivery (*e.g.* drugs, genes, proteins, and peptides) and imaging to cell

applications, and specifically stem cell applications related to vascular tissue engineering, would be advantageous.

A recent investigation by Yang et al. reported on a magnetic nanovector that can ensure simultaneous *in vitro* gene delivery to hMSCs and their magnetic cell labeling for *in vivo* tracking after transplantation, as shown in Fig. 3B [103]. Magnetic nanovectors (73.7 ± 8.7 nm) were conjugated with eGFP and delivered to hMSCs *in vitro*, and the transfected cells were injected into rats following brain ischemia and monitored using MRI [103]. Another approach related to combined gene delivery and imaging was studied by Zhang et al. [104]. They developed liposomes targeted with an arginine-rich peptide for *in vivo* gene delivery and imaging. The liposomes (100 nm) targeted with short linear peptides (CPRRP and CPPRR) rapidly and efficiently bound to blood vessel walls in the heart following intravenous injection [104]. The liposomes also contained a radiolabeled lipid ([^{18}F]FDP), which allowed for monitoring of the circulation, targeting, and metabolism of the particle using PET [104]. Similar NP systems to Zhang et al. could be implemented for combined drug delivery and imaging by incorporating genes into the NPs targeted to specific cells or tissues.

Multimodal nanoscale scaffolds

Recently, tissue engineers have adopted commonly-used clinical imaging techniques such as ultrasound and MRI in order to monitor time-lapse accumulation of biomolecules *in vitro* inside a tissue-engineered environment [105]. To evaluate ECM accumulation in a cell-seeded fibrin scaffold during cultivation, Kreitz et al. utilized gray-scale values to correlate with the amount of hydroxyproline, which is one of the components in collagen, following 13 MHz ultrasound imaging [105]. However, this approach does not seem to specifically map increased or decreased amounts of multiple biomolecules synthesized by cells.

Visualizing a tissue-engineered blood vessel can be approached by fabricating scaffolds using materials with incorporated contrast agents or light-sensitive materials. Cunha-Reis et al. suggested a direct material-based monitoring strategy could be promising to directly visualize morphological changes of implanted scaffolds *in vivo* [106]. Using tetramethylrhodamine isothiocyanate (TRITC), a commonly used fluorescent dye in immunocytochemistry, the fluorescent intensity from a chitosan membrane (80 μm thickness) can be monitored using confocal microscopy over time to demonstrate a linear correlation with weight loss [106]. Cai et al. reported direct photoacoustic imaging (acoustic and optical resolution) of biodegradable porous PLGA scaffolds, which were located in blood or muscle tissue without cell labeling [107]. This was possible because the PLGA included single-wall nanotubes (diameter = 1–2 nm) as a signal booster [107]. In addition, Yang et al. suggested a novel fluorescent biomaterial as a next-generation multifunctional scaffold material by demonstrating its photoluminescent imaging capacity via *in vitro* cell and *in vivo* nude mouse injection studies (Fig. 3C) [108]. This concept is that poly(octamethylene citrates) crosslinked with specific amino acids, such as serine or cysteine, can show specific excitation/emission/quantum yield levels: *i.e.*, 290–660 nm/303–725 nm/26% with serine and 240–420 nm/312–561 nm/62.3% with cysteine, respectively [108]. Bull et al. developed self-assembled peptides that form spherical and fiber-like

nanostructures (6–8 nm in diameter) which are coupled to a modified MRI agent (Gd(III)) [109]. The gel scaffolds could potentially be tracked *in vivo* using MRI in order to detect their fate, migration and degradation [109]. The self-assembling peptide amphiphiles have previously been used as scaffolds for regenerative medicine, and thus this system could possibly be extended to vascular tissue engineering applications.

A coaxial-electrospun scaffold has been reported by Yang et al. with a self-light emissive system that can generate electroluminescence from triple-layers of (1) metal core, (2) ruthenium (II) tris (bipyridine) (Ru $(bpy)_3)^{2+}$ $(PF_6)^-)_2)$ and poly(ethyl oxide), and (3) indium—tin oxide [110]. These layers serve as cathode, ionic charging space, and anode, respectively [110]. These dual-functional scaffolds could potentially have a more stable imaging signal without significant cytotoxicity issues compared to cell-mediated imaging. This is attributed to the scaffolds' mechanical properties, biocompatibility, and biodegradability, all of which have been optimized depending on specific tissue qualifications [108,110]. As a vascular tissue scaffold, Ito et al. developed triple layers made of blood vessel cells having 10 nm magnetite NPs (Fe_3O_4) in liposomes on and around a cylindrical magnet [111]. This scaffold system has the potential to combine diverse nanostrategies including scaffolding/cell seeding, biomedical imaging, and delivery systems.

Cells which are magnetically labeled can be directed to desirable locations within scaffolds using magnetic forces. In a study conducted by Shimizu et al., fibroblast cells were magnetically labeled using cationic liposomes containing 10 nm magnetite NPs [112]. The fibroblast cells were then driven to a decellularized common carotid artery using magnetic force and attached at 99% efficiency. This study demonstrates the application of magnetically seeding cells onto decelluarized scaffolds for vascular tissue applications. Furthermore, the magnetically labeled cell/scaffold construct could potentially be imaged and tracked *in vivo* using MRI. Moreover, an automatic bioprinting system with NPs for blood vessel scaffolds can be an attractive scaffolding technique, which has great potential for scalability [113]. Multifunctional nanoscaffolds could be employed which are capable of uniform or specific cell environmental control by patterning, carrying bioactive molecules, and imaging based on contrast agent-like properties [113]. Buyukhatipoglu et al. utilized a bioprinting technique and 20–40 nm NanoArc magnetic iron oxide NPs to seed cells and fabricate patterned surfaces in alginate as an artificial vascular guidance conduit [113]. Cell viability is still a challenge as EC viability decreased with NPs and pressure [113]. Mechanical properties of combined scaffolds depended on fabrication parameters such as concentration and size of NPs, and gel concentration [113].

Conclusion and future prospects: Multifunctional vascular regenerative nanomedicine

Beyond vascular grafting, an efficient artificial guidance for neovascularization in a tissue-engineered system is one of the most difficult tasks for biomedical researchers. To construct a superior microvascular network, the actions and roles of blood vessel cells (*e.g.* ECs and pericytes), scaffolds, and bioactive molecules should be synchronized spatiotemporally. The current review describes how the combined manipulation of prior well-developed nanoscale

technologies in biomaterial engineering, biomedical imaging, and gene/cell delivery can pioneer a next-generation biomedical field to enhance blood vessel regeneration. The multifunctionalized scaffolds can give guidance for regenerative cells to attach, proliferate and stimulate their bioactivity in a tissue of interest by incorporating appropriate bioactive molecule release systems. Moreover, the time-lapse changes of implanted scaffolds or seeded cells' behaviors *in vitro* or *in vivo* can be monitored by utilizing imaging contrast agents including self-light emitting biomaterials.

However, in spite of important progress in regenerative nanomedicine, there are still critical challenges for an advanced nanomedical approach to develop a clinical device. First of all, it may be necessary to mimic much of the complex, natural regenerative processes in order to repair diseased or damaged tissue. For example, skin wound healing occurs with several ordered events including coagulation, vasodilation, inflammation, epithelialization, and angiogenesis. Mismatch between required time-specific cues for healing and parameters of exogenously delivered bioactive molecules (*e.g.* types, amounts, and release timing) might not induce superior regeneration outcomes. Therefore, nanoscale materials should be designed according to the time-dependent requirements of target tissues to be regenerated in order to maximize the tissue-healing capacity of nano-devices. Secondly, we need to comply with tissue-specific characteristics, such as mechanical properties and structures. Hence, a tissue-engineered device must be tailored to the target tissue area and function. Furthermore, for a combined nanostrategy, such as electrospun nanofibers releasing angiogenic growth factors, the dual/multi-functional material should be designed to satisfy two different purposes, *e.g.*, scaffolding and controlled delivery. Consequently, there may exist design trade-offs among various material parameters such as degradation, elasticity, porosity, strength, and cytotoxicity depending on the expected roles (*i.e.*, scaffolding, imaging, and delivering) of nanostrategies.

We believe this review will (1) introduce regenerative nanomedicine strategies focused on blood vessel regeneration, (2) suggest a nanotechnology approach to solve critical challenges and (3) present a number of novel nanoscale techniques that have been developed in other fields, such as cancer and pharmaceutical research, into vascular tissue engineering.

Biographies

Eunna Chung, Ph.D. Dr. Eunna Chung received her Ph.D. in the School of Biomedical Sciences and Engineering at Virginia Tech in 2010. She joined the Laboratory of Cardiovascular Tissue Engineering (P.I.: Dr. Suggs) in the department of Biomedical Engineering at The University of Texas at Austin (UT Austin) as a postdoctoral fellow in

2011. Her current research at UT Austin is focused on developing a novel imaging-capable burn dressing material using adipose-derived stem cells and gold nanoparticles for skin and blood vessel regeneration.

Laura M. Ricles received her B.S. in Bioengineering from Lehigh University in 2009. She is currently pursuing her Ph.D. in Biomedical Engineering at The University of Texas at Austin under the supervision of Dr. Laura Suggs and Dr. Stanislav Emelianov, where she is a National Science Foundation Graduate Research Fellow and Thrust 2000 Fellow. Her research focuses on nanoparticle labeling of cells, cell tracking, and stem cell therapy related to vascular repair.
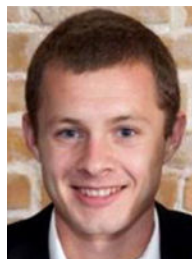
Ryan S. Stowers received his B.S. degree in Bioengineering from Clemson University in 2009. He is currently pursuing a Ph.D. in Biomedical Engineering at The University of Texas at Austin in the laboratory of Laura Suggs. His research focuses on developing tunable hydrogels to mimic dynamic characteristics of the extracellular matrix during disease or development.

Seung Yun Nam received his B.S. in Electrical and Computer Engineering from Seoul National University, South Korea, in 2007. He entered The University of Texas at Austin for his graduate education, and received his M.S. degree in Electrical and Computer Engineering (Biomedical Engineering track) in 2010. Currently he is pursuing his Ph.D. under the supervision of Dr. Stanislav Emelianov at The University of Texas at Austin. His

graduate research has been focused on monitoring stem cells and tissue regeneration using molecular contrast agents and combined ultrasound and photoacoustic imaging.

Stanislav Y. Emelianov, Ph.D. (B.S. and Ph.D. from The Moscow State University, Russia) is currently a Professor and an Associate Chair for Research in the Department of Biomedical Engineering at The University of Texas at Austin where he directs the Ultrasound Imaging and Therapeutics Research Laboratory. In addition, Dr. Emelianov is an Adjunct Professor of Imaging Physics at The University of Texas M.D. Anderson Cancer Center in Houston. Dr. Emelianov's research interests are in the areas of medical imaging for diagnostic and therapeutic applications, bionanotechnology, photoacoustic imaging, ultrasound imaging, elasticity imaging, cellular/molecular imaging, and functional imaging.

Laura J. Suggs, Ph.D. Dr. Laura Suggs is currently an Associate Professor in Biomedical Engineering at The University of Texas at Austin. She earned her Ph.D. in chemical engineering with a concentration in biomaterials and tissue engineering from Rice University in 1998. She joined the faculty of UT Austin in 2004. In 2002, she received the National Science Foundation's Advance Fellowship for outstanding female faculty and a CAREER award in 2009. Her laboratory is focused on stem cells and regenerative medicine in cardiovascular applications and in particular with controllable microenvironments for stem cell engineering.

Abbreviations

ADSC	adipose-derived stem cell
bFGF	basic fibroblast growth factor
BMSC	bone marrow-derived mesenchymal stem cell
BSA	bovine serum albumin
CT	computed tomography

EC	endothelial cell
ECM	extracellular matrix
eGFP	enhanced green fluorescent protein
eNOS	endothelial nitric oxide synthase
EPC	endothelial progenitor cell
ESC	embryonic stem cell
FGF-2	fibroblast growth factor-2
FITC	fluorescein isothiocyanate
hCNS-SC	human central nervous system stem cell
HGF	hepatocyte growth factor
HIF-1α	hypoxia-inducible factor-1α
HUVEC	human umbilical vein endothelial cell
Hu-uPA	human urokinase plasminogen activator
MMP	matrix metalloproteinase
MI	myocardial infarction
MRI	magnetic resonance imaging
MSC	mesenchymal stem cell
MTOC	microtubule organizing centers
NGF	nerve growth factor
NP	nanoparticle
PA	peptide amphiphile
PAMAM	polyamidoamine
PCL	polycaprolactone
PDGF	platelet-derived growth factor
PDMS	poly(dimethylsiloxane)
PEG	polyethylene glycol
PEI	polyethylenimine
PET	positron emission tomography
PLCL	poly(L-lactide-co-ε-caprolactone)

PLGA	poly(lactic-co-glycolic acid)
PLLA	poly(L-lactic acid)
PMMA	poly(methyl methacrylate)
PVA	polyvinyl alcohol
Q11	Ac-QQKFQFQFEQQ-Am
QD	quantum dot
RAEC	rat aortic endothelial cell
RGD	arginineglycine-aspartic acid
SA	self assembly
SC-PEG	difunctional succinimidyl carbonate-polyethylene glycol
SMC	smooth muscle cell
SPECT	single-photon emission computed tomography
SPIO	superparamagnetic iron oxide
TGF-β1	transforming growth factor-beta 1
TRITC	tetramethylrhodamine isothiocyanate
VEGF	vascular endothelial growth factor

References

1. Wagner V, Dullaart A, Bock AK, Zweck A. Nat Biotechnol. 2006; 24:1211–1217. [PubMed: 17033654]

2. Lin S, Xie X, Patel MR, Yang YH, Li Z, Cao F, Gheysens O, Zhang Y, Gambhir SS, Rao JH, Wu JC. BMC Biotechnol. 2007; 7:67. [PubMed: 17925032]

3. Ricles LM, Nam SY, Sokolov K, Emelianov SY, Suggs LJ. Int J Nanomed. 2011; 6:407–416.

4. Nam SY, Ricles LM, Suggs LJ, Emelianov SY. PLoS ONE. 2012; 7:e37267. [PubMed: 22615959]

5. Lange C, Togel F, Ittrich H, Clayton F, Nolte-Ernsting C, Zander AR, Westenfelder C. Kidney Int. 2005; 68:1613–1617. [PubMed: 16164638]

6. Davani S, Marandin A, Mersin N, Royer B, Kantelip B, Herve P, Etievent JP, Kantelip JP. Circulation. 2003; 108(Suppl 1):II253–II258. [PubMed: 12970242]

7. Tamama K, Sen CK, Wells A. Stem Cells Dev. 2008; 17:897–908. [PubMed: 18564029]

8. Wang C, Yin S, Cen L, Liu Q, Liu W, Cao Y, Cui L. Tissue Eng Part A. 2010; 16:1201–1213. [PubMed: 19895205]

9. Marino G, Rosso F, Ferdinando P, Grimaldi A, De Biasio G, Cafiero G, Barbarisi M, Barbarisi A. J Biomed Mater Res A. 2012; 100:543–548. [PubMed: 22162251]

10. Fan CL, Li Y, Gao PJ, Liu JJ, Zhang XJ, Zhu DL. Acta Pharmacol Sin. 2003; 24:212–218. [PubMed: 12617768]

11. Sone M, Itoh H, Yamahara K, Yamashita JK, Yurugi-Kobayashi T, Nonoguchi A, Suzuki Y, Chao TH, Sawada N, Fukunaga Y, Miyashita K, Park K, Oyamada N, Taura D, Tamura N, Kondo Y, Nito S, Suemori H, Nakatsuji N, Nishikawa S, Nakao K. Arteriosc Thromb Vasc Biol. 2007; 27:2127–2134.

12. Dvir T, Timko BP, Kohane DS, Langer R. Nat Nanotechnol. 2011; 6:13–22. [PubMed: 21151110]

13. Tsang KY, Cheung MC, Chan D, Cheah KS. Cell Tissue Res. 2010; 339:93–110. [PubMed: 19885678]

14. Hynes RO. Science. 2009; 326:1216–1219. [PubMed: 19965464]

15. Zhang G, Drinnan CT, Geuss LR, Suggs LJ. Acta Biomater. 2010; 6:3395–3403. [PubMed: 20302976]

16. Mironov V, Kasyanov V, Markwald RR. Trends Biotechnol. 2008; 26:338–344. [PubMed: 18423666]

17. Perumcherry SR, Chennazhi KP, Nair SV, Menon D, Afeesh R. Tissue Eng Part C Methods. 2011; 17:1121–1130. [PubMed: 21902615]

18. Hajiali H, Shahgasempour S, Naimi-Jamal MR, Peirovi H. Int J Nanomed. 2011; 6:2133–2141.

19. Ma PX, Zhang R. J Biomed Mater Res. 1999; 46:60–72. [PubMed: 10357136]

20. Ma Z, Kotaki M, Inai R, Ramakrishna S. Tissue Eng. 2005; 11:101–109. [PubMed: 15738665]

21. Webber MJ, Kessler JA, Stupp SI. J Int Med. 2010; 267:71–88.

22. Matson JB, Zha RH, Stupp SI. Curr Opin Solid State Mater Sci. 2011; 15:225–235. [PubMed: 22125413]

23. Rajangam K, Arnold MS, Rocco MA, Stupp SI. Biomaterials. 2008; 29:3298–3305. [PubMed: 18468676]

24. Jung JP, Jones JL, Cronier SA, Collier JH. Biomaterials. 2008; 29:2143–2151. [PubMed: 18261790]

25. Cho H, Balaji S, Sheikh AQ, Hurley JR, Tian YF, Collier JH, Crombleholme TM, Narmoneva DA. Acta Biomater. 2012; 8:154–164. [PubMed: 21925628]

26. Sagnella SM, Kligman F, Anderson EH, King JE, Murugesan G, Marchant RE, Kottke-Marchant K. Biomaterials. 2004; 25:1249–1259. [PubMed: 14643599]

27. Tambralli A, Blakeney B, Anderson J, Kushwaha M, Andukuri A, Dean D, Jun HW. Biofabrication. 2009; 1:025001. [PubMed: 20811101]

28. Narmoneva DA, Vukmirovic R, Davis ME, Kamm RD, Lee RT. Circulation. 2004; 110:962–968. [PubMed: 15302801]

29. Davis ME, Motion JP, Narmoneva DA, Takahashi T, Hakuno D, Kamm RD, Zhang S, Lee RT. Circulation. 2005; 111:442–450. [PubMed: 15687132]

30. Lu J, Rao MP, MacDonald NC, Khang D, Webster TJ. Acta Biomater. 2008; 4:192–201. [PubMed: 17851147]

31. Fine E, Zhang L, Fenniri H, Webster TJ. Int J Nanomed. 2009; 4:91–97.

32. Dalby MJ, Riehle MO, Johnstone H, Affrossman S, Curtis AS. Biomaterials. 2002; 23:2945–2954. [PubMed: 12069336]

33. Wang GJ, Lin YC, Hsu SH. Biomed Microdev. 2010; 12:841–848.

34. Yim EK, Reano RM, Pang SW, Yee AF, Chen CS, Leong KW. Biomaterials. 2005; 26:5405–5413. [PubMed: 15814139]

35. Miller DC, Thapa A, Haberstroh KM, Webster TJ. Biomaterials. 2004; 25:53–61. [PubMed: 14580908]

36. Chung TW, Liu DZ, Wang SY, Wang SS. Biomaterials. 2003; 24:4655–4661. [PubMed: 12951008]

37. Hadjizadeh A, Doillon CJ. J Tissue Eng Regen Med. 2010; 4:524–531. [PubMed: 20872739]

38. Bettinger CJ, Zhang Z, Gerecht S, Borenstein JT, Langer R. Adv Mater. 2008; 20:99–103. [PubMed: 19440248]

39. Liliensiek SJ, Wood JA, Yong J, Auerbach R, Nealey PF, Murphy CJ. Biomaterials. 2010; 31:5418–5426. [PubMed: 20400175]

40. Schroeder T. Nature. 2008; 453:345–351. [PubMed: 18480816]

41. Weissleder R, Pittet MJ. Nature. 2008; 452:580–589. [PubMed: 18385732]

42. Folarin AA, Konerding MA, Timonen J, Nagl S, Pedley RB. Microvasc Res. 2010; 80:89–98. [PubMed: 20303995]

43. Hashizume H, Baluk P, Morikawa S, McLean JW, Thurston G, Roberge S, Jain RK, McDonald DM. Am J Pathol. 2000; 156:1363–1380. [PubMed: 10751361]

44. McDonald DM, Choyke PL. Nat Med. 2003; 9:713–725. [PubMed: 12778170]

45. Nanz D, Weishaupt D, Quick HH, Debatin JF. Magn Reson Med. 2000; 43:645–648. [PubMed: 10800028]

46. Christoforidis GA, Yang M, Kontzialis MS, Larson DG, Abduljalil A, Basso M, Yang W, Ray-Chaudhury A, Heverhagen J, Knopp MV, Barth RF. Invest Radiol. 2009; 44:375–383. [PubMed: 19448552]

47. Howles GP, Ghaghada KB, Qi Y, Mukundan S Jr, Johnson GA. Magn Reson Med. 2009; 62:1447–1456. [PubMed: 19902507]

48. Lu W, Huang Q, Ku G, Wen X, Zhou M, Guzatov D, Brecht P, Su R, Oraevsky A, Wang LV, Li C. Biomaterials. 2010; 31:2617–2626. [PubMed: 20036000]

49. Winter PM, Caruthers SD, Allen JS, Cai K, Williams TA, Lanza GM, Wickline SA. Magn Reson Med. 2010; 64:369–376. [PubMed: 20665780]

50. Smith BR, Cheng Z, De A, Koh AL, Sinclair R, Gambhir SS. Nano Lett. 2008; 8:2606–2659.

51. Michalet X. Science. 2005; 307:538–544. [PubMed: 15681376]

52. So MK, Xu C, Loening AM, Gambhir SS, Rao J. Nat Biotechnol. 2006; 24:339–343. [PubMed: 16501578]

53. Muller-Borer BJ, Collins MC, Gunst PR, Cascio WE, Kypson AP. J Nanobiotechnol. 2007; 5:9–17.

54. Hardman R. Environ Health Perspect. 2006; 114:165–172. [PubMed: 16451849]

55. Lévy R, Shaheen U, Cesbron Y, Sée V. Nano Rev. 2010; 1:4889.

56. Alkilany AM, Murphy CJ. J Nanopart Res. 2010; 12:2313–2333. [PubMed: 21170131]

57. Chen P, Mwakwari S, Oyeler A. Nanotechnol Sci Appl. 2008; 1:45–66. [PubMed: 24198460]

58. Ghosh P, Han G, De M, Kim C, Rotello V. Adv Drug Deliv Rev. 2008; 60:1307–1315. [PubMed: 18555555]

59. Solanki A, Kim J, Lee KB. Nanomedicine. 2008; 3:567–578. [PubMed: 18694318]

60. Mallidi S, Larson T, Tam J, Joshi PP, Karpiouk A, Sokolov K, Emelianov S. Nano Lett. 2009; 9:2825–2831. [PubMed: 19572747]

61. Homan K, Shah J, Gomez S, Gensler H, Karpiouk A, Brannon-Peppas L, Emelianov S. J Biomed Opt. 2010; 15:021316. [PubMed: 20459238]

62. Durr NJ, Larson T, Smith DK, Korgel BA, Sokolov K, Ben-Yakar A. Nano Lett. 2007; 7:941–945. [PubMed: 17335272]

63. Nagesha D, Laevsky G, Lampton P, Banyal R, Warner C, DiMarzio C, Sridhar S. Int J Nanomed. 2007; 2:813–819.

64. Kubinová Š, Syková E. Min Invas Ther Allied Technol. 2010; 19:144–156.

65. Ferreira L, Karp J, Nobre L, Langer R. Cell Stem Cell. 2008; 3:136–146. [PubMed: 18682237]

66. Guzman R, Uchida N, Bliss TM, He D, Christopherson KK, Stellwagen D, Capela A, Greve J, Malenka RC, Moseley ME, Palmer TD, Steinberg GK. Proc Natl Acad Sci U S A. 2007; 104:10211–10216. [PubMed: 17553967]

67. Kraitchman DL, Heldman AW, Atalar E, Amado LC, Martin BJ, Pittenger MF, Hare JM, Bulte JW. Circulation. 2003; 107:2290–2293. [PubMed: 12732608]

68. Lu CW, Hung Y, Hsiao JK, Yao M, Chung TH, Lin YS, Wu SH, Hsu SC, Liu HM, Mou CY, Yang CS, Huang DM, Chen YC. Nano Lett. 2006; 7:149–154.

69. Narayanan S, Sathy BN, Mony U, Koyakutty M, Nair SV, Menon D. ACS Appl Mater Interfaces. 2012; 4:251–260. [PubMed: 22103574]

70. Patel D, Kell A, Simard B, Deng JX, Xiang B, Lin HY, Gruwel M, Tian GH. Biomaterials. 2010; 31:2866–2873. [PubMed: 20053440]

71. Hung HS, Chen HC, Tsai CH, Lin SZ. Cell Transplant. 2011; 20:63–70. [PubMed: 20887685]

72. Bleiziffer O, Eriksson E, Yao F, Horch RE, Kneser U. J Cell Mol Med. 2007; 11:206–223. [PubMed: 17488473]

73. Spadaccio C, Chello M, Trombetta M, Rainer A, Toyoda Y, Genovese JA. J Cell Mol Med. 2009; 13:422–439. [PubMed: 19379142]

74. Harris TJ, Green JJ, Fung PW, Langer R, Anderson DG, Bhatia SN. Biomaterials. 2010; 31:998–1006. [PubMed: 19850333]

75. Kulkarni M, Greiser U, O'Brien T, Pandit A. Trends Biotechnol. 2010; 28:28–36. [PubMed: 19896228]

76. Sharif F, Hynes SO, McCullagh KJ, Ganley S, Greiser U, McHugh P, Crowley J, Barry F, O'Brien T. Gene Ther. 2012; 19:321–328. [PubMed: 21716298]

77. Trentin D, Hall H, Wechsler S, Hubbell JA. Proc Natl Acad Sci U S A. 2006; 103:2506–2511. [PubMed: 16477043]

78. Zaitsev S, Cartier R, Vyborov O, Sukhorukov G, Paulke BR, Haberland A, Parfyonova Y, Tkachuk V, Bottger M. Pharm Res. 2004; 21:1656–1661. [PubMed: 15497693]

79. Asahara T. Handbook Exp Pharmacol. 2007; 180:181–194.

80. Deng WW, Cao X, Wang M, Qu R, Su WY, Yang Y, Wei YW, Xu XM, Yu JN. Int J Nanomed. 2012; 7:1297–1311.

81. Yang F, Cho SW, Son SM, Bogatyrev SR, Singh D, Green JJ, Mei Y, Park S, Bhang SH, Kim BS, Langer R, Anderson DG. Proc Natl Acad Sci U S A. 2010; 107:3317–3322. [PubMed: 19805054]

82. Zhu K, Guo C, Lai H, Yang W, Xia Y, Zhao D, Wang C. J Mater Sci Mater Med. 2011; 22:2477–2485. [PubMed: 21870080]

83. Negishi Y, Endo-Takahashi Y, Matsuki Y, Kato Y, Takagi N, Suzuki R, Maruyama K, Aramaki Y. Mol Pharm. 2012; 9:1834–1840. [PubMed: 22571418]

84. Huang M, Vitharana SN, Peek LJ, Coop T, Berkland C. Biomacromolecules. 2007; 8:1607–1614. [PubMed: 17428030]

85. Golub JS, Kim YT, Duvall CL, Bellamkonda RV, Gupta D, Lin AS, Weiss D, Taylor W Robert, Guldberg RE. Am J Physiol Heart Circ Physiol. 2010; 298:H1959–H1965. [PubMed: 20228260]

86. Zhang J, Postovit LM, Wang D, Gardiner RB, Harris R, Abdul M, Thomas A. Nanoscale Res Lett. 2009; 4:1297–1302. [PubMed: 20628467]

87. Jeon O, Kang SW, Lim HW, Chung J Hyung, Kim BS. Biomaterials. 2006; 27:1598–1607. [PubMed: 16146647]

88. d'Angelo I, Garcia-Fuentes M, Parajo Y, Welle A, Vantus T, Horvath A, Bokonyi G, Keri G, Alonso MJ. Mol Pharm. 2010; 7:1724–1733. [PubMed: 20681555]

89. Ji W, Sun Y, Yang F, van den Beucken JJ, Fan M, Chen Z, Jansen JA. Pharm Res. 2011; 28:1259–1272. [PubMed: 21088985]

90. Kim MS, Shin YM, Lee JH, Kim SI, Nam YS, Shin CS, Shin H. Macromol Biosci. 2011; 11:122–130. [PubMed: 20886548]

91. Zhang YZ, Wang X, Feng Y, Li J, Lim CT, Ramakrishna S. Biomacromolecules. 2006; 7:1049–1057. [PubMed: 16602720]

92. Liao IC, Chew SY, Leong KW. Nanomedicine (Lond). 2006; 1:465–471. [PubMed: 17716148]

93. Lu Y, Jiang H, Tu K, Wang L. Acta Biomater. 2009; 5:1562–1574. [PubMed: 19251494]

94. Sahoo S, Ang LT, Goh JC, Toh SL. J Biomed Mater Res A. 2010; 93:1539–1550. [PubMed: 20014288]

95. Drinnan CT, Zhang G, Alexander MA, Pulido AS, Suggs LJ. J Control Release. 2010; 147:180–186. [PubMed: 20381553]

96. Sun Q, Silva EA, Wang A, Fritton JC, Mooney DJ, Schaffler MB, Grossman PM, Rajagopalan S. Pharm Res. 2010; 27:264–271. [PubMed: 19953308]

97. Tan Q, Tang H, Hu J, Hu Y, Zhou X, Tao Y, Wu Z. Int J Nanomed. 2011; 6:929–942.

98. Breen A, Dockery P, O'Brien T, Pandit A. J Biomed Mater Res A. 2009; 89:876–884. [PubMed: 18465822]

99. Kulkarni M, Breen A, Greiser U, O'Brien T, Pandit A. Biomacromolecules. 2009; 10:1650–1654. [PubMed: 19385658]

100. Chow LW, Bitton R, Webber MJ, Carvajal D, Shull KR, Sharma AK, Stupp SI. Biomaterials. 2011; 32:1574–1582. [PubMed: 21093042]

101. Ferreira LS, Gerecht S, Fuller J, Shieh HF, Vunjak-Novakovic G, Langer R. Biomaterials. 2007; 28:2706–2717. [PubMed: 17346788]

102. Cheng YCS, Meyers AJD, Panagopoulos I, Fei B, Burda C. J Am Chem Soc. 2008; 130:10643–10647. [PubMed: 18642918]

103. Yang J, Lee ES, Noh MY, Koh SH, Lim EK, Yoo AR, Lee K, Suh JS, Kim SH, Haam S, Huh YM. Biomaterials. 2011; 32:6174–6182. [PubMed: 21696819]

104. Zhang H, Kusunose J, Kheirolomoom A, Seo JW, Qi J, Watson KD, Lindfors HA, Ruoslahti E, Sutcliffe JL, Ferrara KW. Biomaterials. 2008; 29:1976–1988. [PubMed: 18255141]

105. Kreitz S, Dohmen G, Hasken S, Schmitz-Rode T, Mela P, Jockenhoevel S. Tissue Eng Part C Methods. 2011; 17:1021–1026. [PubMed: 21663456]

106. Cunha-Reis C, El Haj AJ, Yang X, Yang Y. J Tissue Eng Regen Med. 2011; 5:770–779. [PubMed: 22002920]

107. Cai X, Paratala BS, Hu S, Sitharaman B, Wang LV. Tissue Eng Part C Methods. 2012; 18:310–317. [PubMed: 22082018]

108. Yang J, Zhang Y, Gautam S, Liu L, Dey J, Chen W, Mason RP, Serrano CA, Schug KA, Tang L. Proc Natl Acad Sci U S A. 2009; 106:10086–10091. [PubMed: 19506254]

109. Bull SR, Guler MO, Bras RE, Meade TJ, Stupp SI. Nano Lett. 2005; 5:1–4. [PubMed: 15792402]

110. Yang H, Lightner CR, Dong L. ACS Nano. 2012; 6:622–628. [PubMed: 22196130]

111. Ito A, Ino K, Hayashida M, Kobayashi T, Matsunuma H, Kagami H, Ueda M, Honda H. Tissue Eng. 2005; 11:1553–1561. [PubMed: 16259609]

112. Shimizu K, Ito A, Arinobe M, Murase Y, Iwata Y, Narita Y, Kagami H, Ueda M, Honda H. J Biosci Bioeng. 2007; 103:472–478. [PubMed: 17609164]

113. Buyukhatipoglu K, Jo W, Sun W, Clyne AM. Biofabrication. 2009; 1:035003. [PubMed: 20811107]
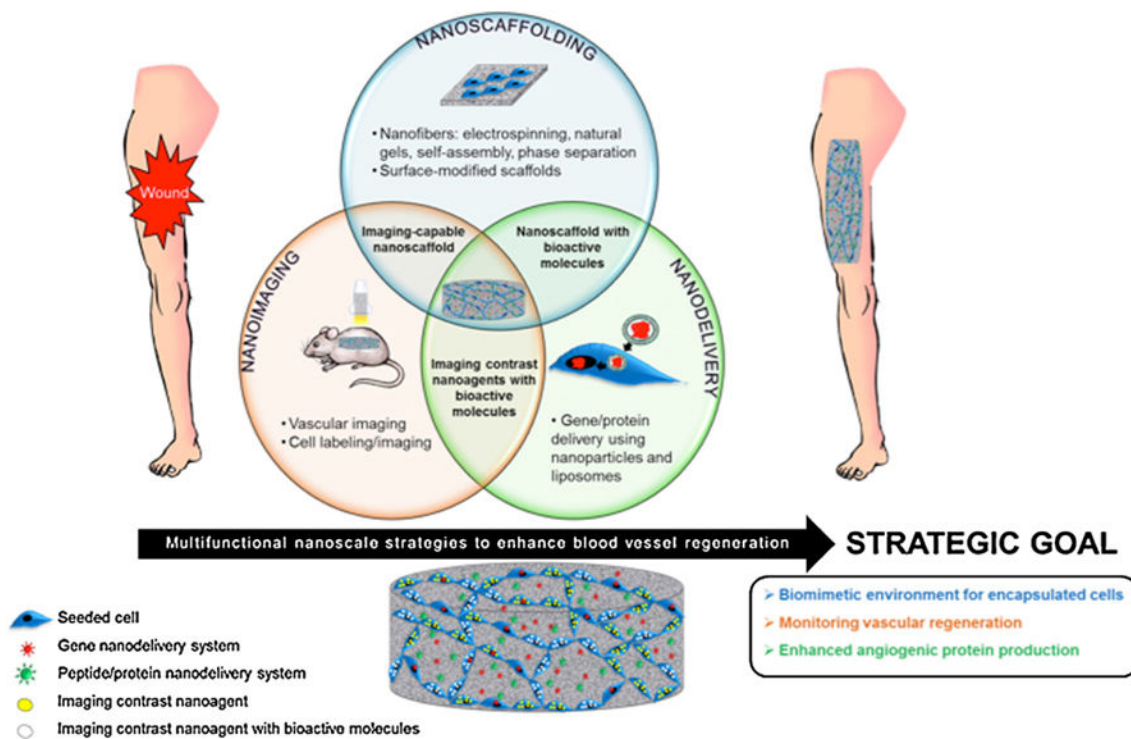
Fig. 1.
Multifunctional nanoscale strategies, including scaffolding, imaging, and bioactive molecule delivery systems for vascular tissue engineering. Nanoscaffolding, nanoimaging, and nanodelivery, as well as the overlap among these three areas (imaging-capable nanoscaffolds, nanoscaffolds with bioactive molecules, and nanoscale contrast agents with bioactive molecules), can be implemented to enhance blood vessel regeneration. The end goal of these three areas is to create a biomimetic environment for encapsulated cells to be delivered to a wound site, monitor the process of vascular regeneration *in vivo*, and enhance angiogenic protein production through gene, peptide, or protein delivery. Seeded cells (blue) can take up contrast agents (yellow) alone or with bioactive molecules (white). These agents also can be incorporated with a nanoscale gene (red) or protein (green) delivery system in a 3D matrix.
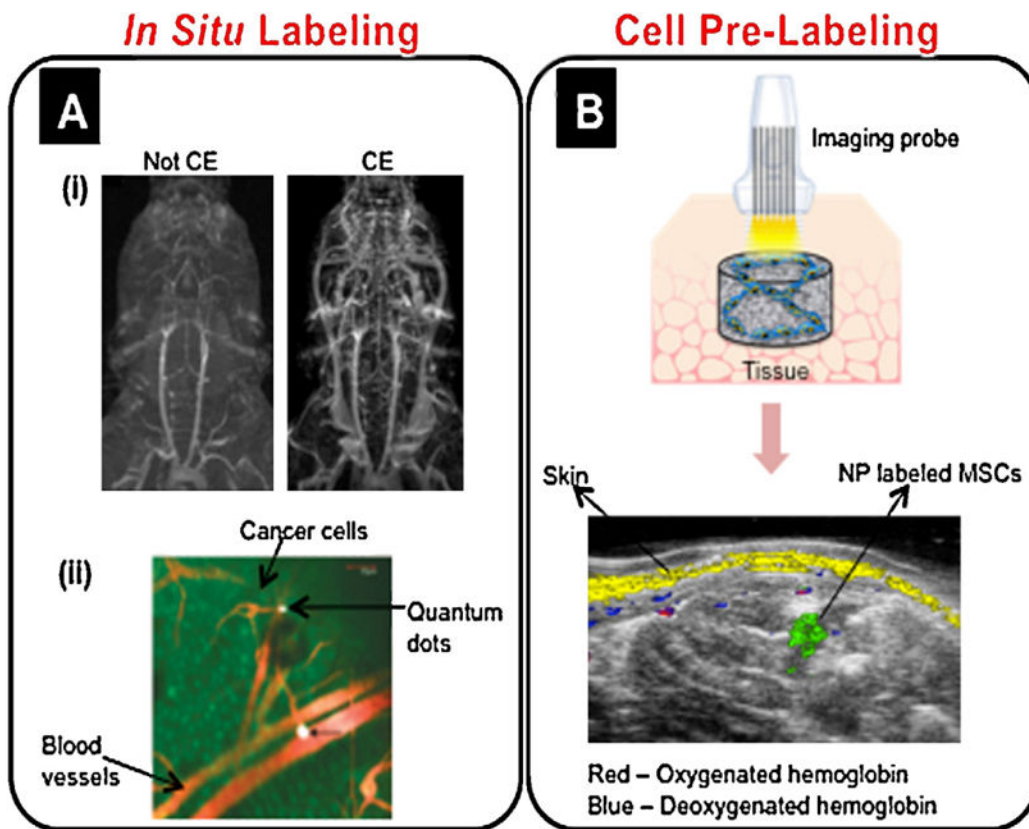
Fig. 2.

Various nanoimaging strategies. (A) *In situ* labeling. (A(i)) Contrast-enhanced (CE) images with a liposomal NP conjugated with gadolinium enabled improved contrast-to-noise ratio, a larger field of view, and imaging of venous structures compared to not contrast-enhanced (Not CE) images [47]. Adapted with permission from [47]. (A(ii)) Intravital imaging demonstrated that RGD-QDs (white) bound to tumor vessel endothelium (red) following injection into an animal model inoculated with EGFP-expressing cancer cells (green) [50]. Adapted with permission from [50]. Copyright 2008 American Chemical Society. (B) Cell pre-labeling. MSCs were pre-labeled with gold NPs, loaded in a PEGylated fibrin gel, and injected intramuscularly into rats. Combined ultrasound and spectroscopic photoacoustic imaging 10 days after injection clearly showed the injected NP labeled stem cells (green), skin (yellow), and oxygenated and deoxygenated hemoglobin (red and blue, respectively) [4].
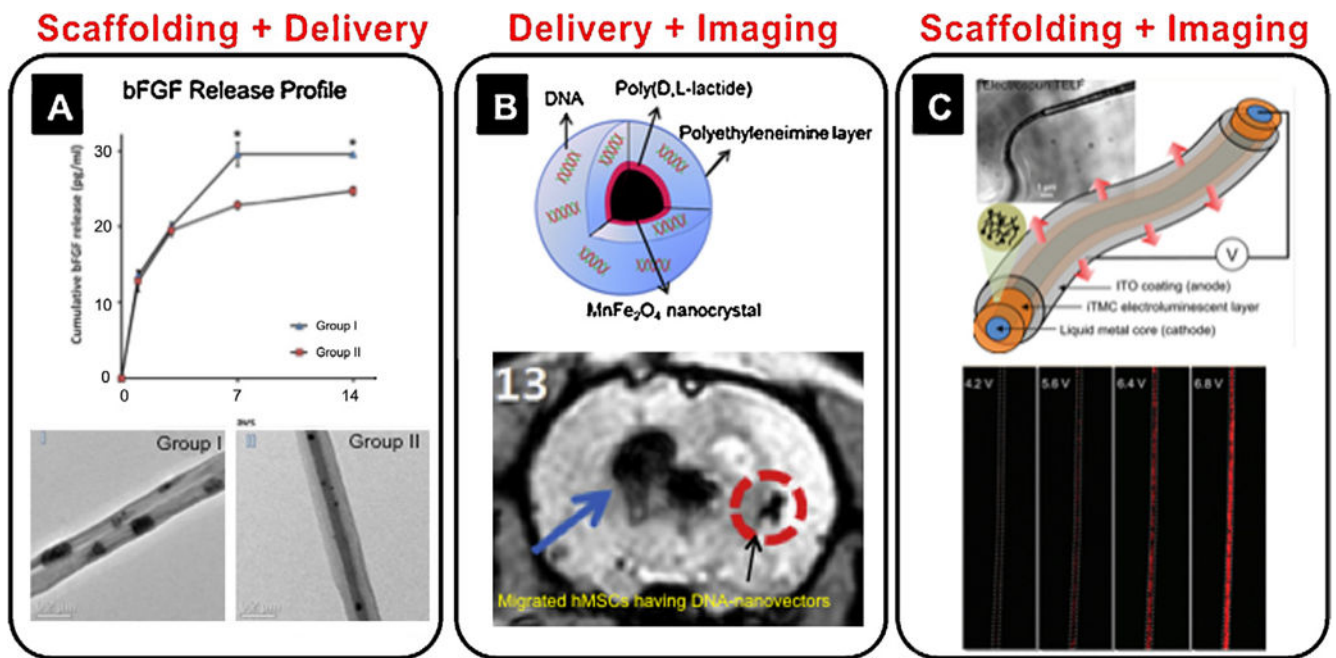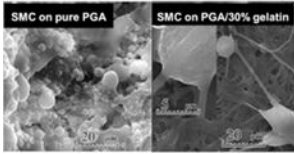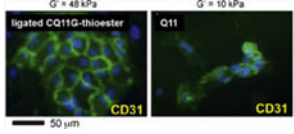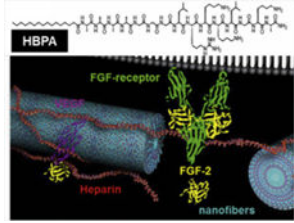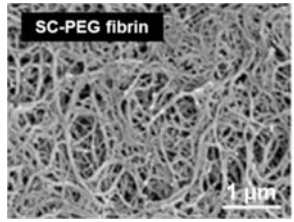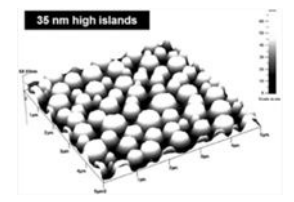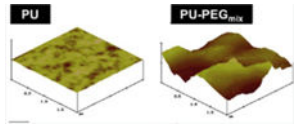
Fig. 3.

Dual-functional nanostrategies. (A) bFGF-loaded electrospun PLGA nanofibers [94]. Mixed PLGA nanofibers with bFGF (group I) and core-shell nanofibers with bFGF (group II) showed different release profiles for bFGF over time. Adapted with permission from [94]. (B) Nanocrystals capable of MRI and DNA delivery into MSCs [103]. Adapted with permission from [103]. MSCs were labeled using eGFP in a MnFeO nanocrystal vector and injected in a rat brain. Fifteen days after occlusion, the MRI signal was acquired away from the original transplanted zone, suggesting the movement of injected eGFP nanovector-traced MSCs. (C) Self-luminescent electrospun nanofibers [110]. Three different layers of nanofibers (ITO, iTMC, and metal core), were used to generate a fluorescent signal. Adapted with permission from [110]. Copyright American Chemical Society.

Table 1

Recent advances of nanoscaffold strategies to induce blood vessel regeneration.
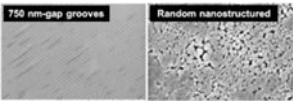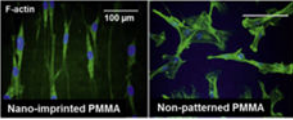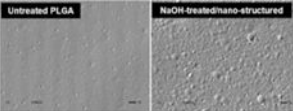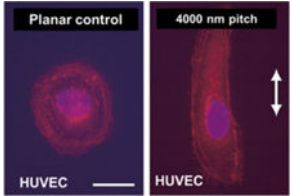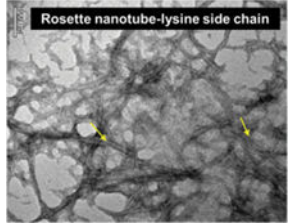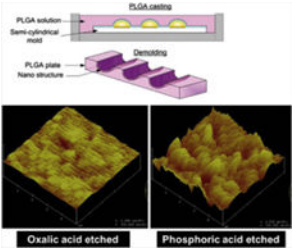
Materials	Nanostructures/cellular morphology	Study model	Outcome	References
Nanoscale-structured vascular scaffolds				
PGA/gelatin nanofiber (87.72 ± 23.34 nm)		*In vitro*	Significantly higher mechanical properties on PGA/gelatin; enhanced EC and SMC growth on PGA with 10% and 30% gelatin, respectively	Hajiali et al.[18]
Self-assembled peptide gel (ligated CQ11*G-thioester, 11–13nm fibrils)		*In vitro*	Greater EC proliferation and CD31expression by the ligated peptide	Jung et al. [24]
Heparin-binding peptide amphiphile (HBPA) nanofibers		*In vitro*	HBPA nanofibers induced superior tubule-like interconnected networks by EC than scrambled PA	Rajangam et al. [23]
PEGylated fibrin (200–400 nm)		*In vitro/in vivo*	Tunable nanofiber diameter and storage modulus based on chemical modification	Zhang et al. [15]
Nanoscale surface-modified vascular scaffold				
Polymer demixed nano-islands (13–95 nm)		*In vitro*	More spread EC morphology depending on altered nanotopography	Dalby et al. [32]
PEG-polyurethane substrates (1.5–40nm)		*In vitro*	Enhanced HUVEC proliferation on higher levels of nanorough surfaces modified with mixed different PEGs	Chung et al. [36]

Materials	Nanostructures/cellular morphology	Study model	Outcome	References
Nanoscale-patterned titanium surfaces (750 nm-100μm space between grooves)		*In vitro*	Significantly enhanced RAEC density at 4 h/1 day on the nanopatterned surface	Lu et al. [30]
Nanopatterned PMMA and PDMS (350 nm linewidth, 700 nm pitch, 350 nm depth)		*In vitro*	Decreased SMC growth on nano-patterned PMMA/PDMS compared to flat surfaces; enhanced MTOC polarization on nano-patterned surfaces	Yim et al. [34]
Nanostructured PLGA		*In vitro*	Significantly increased surface roughness in NaOH-treated and cast PLGA; increased SMC growth but decreased EC growth on treated PLGA	Miller et al. [35]
Nanogrooves in polyurethane (200–2000 nm)		*In vitro*	Organization and alignment of ECs in nanogrooves; differential response based on anatomic origin of ECs	Liliensiek et al. [39]
Titanium stent coated with Rosette nanotube-lysine side chain (3.5 nm diameter)		*In vitro*	Increased EC adherence and proliferation	Fine et al. [31]
Nano-patterned PLGA microvascular scaffolds		*In vitro*	More controlled pattern of EC residence and growth on the 20 nm nanosurface than the 80 nm	Wang et al. [33]

All figures reprinted or adapted with permission.

Table 2

Nanoscale contrast agents used for imaging engineered vasculature.

Imaging modality	Contrast agent	Outcome	Reference
In situ labeling and vascular imaging			
Magnetic resonance imaging	Gadolinium immobilized liposomes (75.9nm)	Increased contrast and larger field of view for imaging small blood vessels	Howles et al. [47]
Photoacoustic imaging	Hollow gold nanospheres (40 nm)	Enhanced vascular contrast and visualization of vessels as small as ~100nm in diameter	Lu et al. [48]
Intravital imaging	RGD-QDs (6–8 nm)	QDs specifically targeted newly formed vessels expressing $\alpha_v\beta_3$ integrins	Smith et al. [50]
Magnetic resonance imaging	Perfluorocarbon NPs (<300 nm)	NPs targeted $\alpha_v\beta_3$ integrins and enhanced angiogenesis for L-arginine treated animals	Winter et al. [49]
Cell pre-labeling and imaging			
Fluorescent microscopy	QDs	QDs detectable up to 2 days or 14 days *in vivo*	Lin et al. [2]
	CdSe/ZnS QDs (10–15 nm)	Dose-dependent cytotoxicity effects on MSCs	Muller-Borer et al. [53]
Photoacoustic imaging	Gold NPs (20–60 nm)	Gold NPs of various sizes and surface coatings did not compromise MSC function	Ricles et al. [3]
	Gold NPs (20 nm)	*In vivo* imaging of MSCs up to day 10	Nam et al. [4]
Multi-photon photoluminescence imaging	Gold NPs (10 nm)	ESC function not compromised and cells were imaged *in vitro*	Nagesha et al. [63]
Magnetic resonance imaging	SPIO	NP labeling had no effect on cell function, and the cells could be tracked *in vivo* up to 18 weeks	Guzman et al. [66]
	Carboxy-dextran-coated iron oxide NPs	MSCs were in the renal cortex up to three days and renal function was significantly improved	Lange et al. [5]
	Poly-L-lysine coated magnetic NPs	MSCs were visible in MI model up to 1 week, but there was significant decrease in signal after 3 weeks	Kraitchman et al. [67]
Magnetic resonance and fluorescence imaging	SPIO@SiO$_2$(FITC)	*In vivo* imaging of MSCs labeled with FITC-incorporated silica-coated core-shell SPIO NPs	Lu et al. [68]
Magnetic resonance imaging and X-ray	Fe$_3$O$_4$/gold nanohybrids (35 nm)	Nanohybrids did not alter cell function and could be imaged with MRI and CT with enhanced contrast	Narayanan et al. [69]
Positron emission tomography and magnetic resonance imaging	SPIO@SiO$_2$	High uptake efficiency of SPIO core NPs in MSCs and no cytotoxic effects	Patel et al. [70]

Table 3

Nanodelivery systems targeting blood vessel regeneration: recent advances.

Materials	Delivered molecules	Fabrication/study model	Outcome	References
Gene delivery				
Hyperbranched polyamidoamine (PAMAM) NPs (100–500 nm)	VEGF	Viral plasmids with hPAMAM NPs, transfection	Higher transfection efficiency into myoblasts; decreased apoptosis until 18 days	Zhu et al. [82]
Peptides-DNA NPs (43–204 nm)	HIF-1α	Peptides-DNA NPs in fibrin	VEGF up-regulation; enhanced angiogenesis	Trentin et al. [77]
Pleurotus eryngii polysaccharide (CPEPs) (80–250 nm)	TGF-β1	A Nonviral vector, CPEPs-TGF-β1 (coacervation) NPs into MSCS	Higher transfection efficiency with low toxicity	Deug et al. [80]
Polyelectrolyte NPs (61.8–169.2 nm)	Hu-uPA	Alternatively charged polyelectrolytes (transfer RNA, the synthetic polyanion polyvinyl sulfate, and the polycation polyethylenimine) into a DNA core; periadventitial administration and rat balloon catheter injury model	Low dose delivery of DNA to blood vessels until 3 days	Zaitsev et al. [78]
Liposome	eNOS	Nonviral gene-eluting stents	Gene delivery at 28 days; improved re-endothelialization; no effect on restenosis	Sharif et al. [76]
Bubble liposomes	bFGF	PEG-modified liposomes with ultrasound contrast gas/ hindlimb ischemia model	Up-regulation of angiogenic genes; higher blood flow	Negishi et al. [83]
Protein delivery				
PLGA NPs (400 nm)	VEGF	Encapsulation, hindlimb ischemia surgery and injection/ mouse femoral artery ligation model	Released 80% by 4 days; increased total vessel volumes/ connectivity	Golub et al. [85]
Heparin/chitosan NPs (67–132 nm)	VEGF	Immobilized NPs to the decelluarized/photooxidized scaffolds	Increased fibroblast infiltration and ECM production; accelerated vascularization	Tan et al. [97]
Polyelectrolyte complex (250 nm)	VEGF	VEGF polyelectrolyte complex including polycations (e.g. chitosan, polyethylenimine, poly-L-lysine) and dextran sulfate	Good encapsulation efficiency (85%); released longer than 10 days	Huang et al. [84]
Mesoporous silica NPs (57 nm)	bFGF	Microemulsed NPs with bFGF	Released for 20 days; HUVEC uptake, no toxicity by 50 µg/ml	Zhang et al. [86]
PLGA-poloxamer NPs (150–200nm)	PDGF, FGF-2	NP encapsulation growth factors (emulsion)	Released for 30 days; no cytotoxicity	D'Angelo et al. [88]
Heparin-conjugated PLGA NPs (100–250nm)	bFGF	bFGF-NPs in fibrin gel	Long release periods (4 weeks); higher microvessel density in mouse ischemic limbs	Jeon et al. [87]